

Structures and melting in infinite gold nanowires

G. Bilalbegović

Department of Physics, University of Rijeka, Omladinska 14, 51000 Rijeka, Croatia

(to be published in Solid State Communications)

Abstract

The temperature dependence of structural properties for infinitely long gold nanowires is studied. The molecular dynamics simulation method and the embedded-atom potential are used. The wires constructed at $T = 0$ K with a face-centered cubic structure and oriented along the (111), (110), and (100) directions are investigated. It was found that multiwalled structures form in all these nanowires. The coaxial cylindrical shells are the most pronounced and well-formed for an initial fcc(111) orientation. The shells stabilize with increasing temperature above 300 K. All nanowires melt at $T < 1100$ K, i.e., well below the bulk melting temperature.

Keywords: A. nanostructures, A. metals, A. surfaces and interfaces, B. nanofabrications, D. phase transitions.

arXiv:cond-mat/0004112v1 [cond-mat.mtrl-sci] 7 Apr 2000

Metallic nanowires are important for applications and for understanding of fundamental properties of materials at nanoscales. Over the past several years investigations on metallic nanowires were devoted mainly to the properties of cylindrical junctions formed between a metallic tip and a metallic substrate [1]. Gold nanostructures whose diameter and length are about 1 *nm* were recently formed in a scanning tunneling microscope and studied by a high-resolution electron microscope [2,3]. Unusual vertical rows of gold atoms were observed. Therefore, it is important to study the internal structure of gold nanowires. Computer simulations are suitable for these investigations.

An important topic in the cluster science is the melting of nanoparticles [4–6]. Experimental, theoretical, and computer simulation studies have shown that the melting temperature depends on the cluster size. These studies suggest the dependence of the form:

$$T_m = T_b - c/R, \quad (1)$$

where T_m is the melting temperature for the spherical nanoparticle of radius R , T_b is the bulk melting temperature, and c is a constant. In recent studies deviations from this law for small sizes are found [5,6]. Melting of clusters, i.e., spherical nanoparticles, was the subject of several recent experiments [6]. In contrast, melting of nanowires was not studied experimentally. The exception is an early work on mercury filaments with diameters between 2 and 10 *nm* [7]. In this experiment a decrease in the melting temperature was detected from the resistance measurements.

It is well known that the presence of geometric (i.e., atomic) and electronic shells determines various properties of clusters [6]. Electronic shells in finite sodium nanowires were recently found in a jellium model calculation [8]. These shells were also observed in the conductance measurements [9]. The Molecular Dynamics (MD) simulation has shown an existence of multishelled finite gold nanowires at room temperature [10]. The cylindrical shells obtained in this simulation resemble geometric shells in clusters. Infinite wires with periodic boundary conditions along the wire axes are more often studied by MD simulations. For example, structures of ultra-thin infinite Pb and Al nanowires at $T = 0$ K were studied by MD simulation [11]. In comparison with finite nanowires, infinite wires are stable in simulations at high temperatures. The MD method was used to investigate premelting of infinite Pb nanowires with the axes along a (110) direction [12]. The size-dependence of melting properties for cylindrical and spherical geometry was compared. It was found that the $1/R$ behavior, as in Eq. (1), approximately holds for a nanowire of radius R . Melting of platinum and silver infinite (100) oriented nanowires was also studied by the MD method [13]. A decrease in the melting temperature was investigated, as well as a change in energy on melting. In Ref. [10] finite gold nanowires with length of up to several *nm* and axes initially oriented only along the (111) direction were investigated at $T = 300$ K. It is also interesting to study infinite gold nanowires. These studies should explain whether multishelled structures appear in infinite wires and starting from other orientations of the axes. Simulations at various temperatures may suggest the optimal method for the fabrication of nanowires. Studies of melting in multiwalled nanowires may also shed light on the role of shells in melting of clusters. In this paper a MD study of the structural and melting properties for infinite gold nanowires is presented. These infinite wires, in comparison with finite gold nanowires in Ref. [10], resemble longer nanowires fabricated in the laboratories. For example, the electron-beam lithography methods nowadays produce metallic nanowires

whose length is $1\mu\text{m}$ and more.

Nanowires were simulated using the classical MD method. The embedded-atom potential with proven reliability for modeling properties of gold was employed [14]. Several fcc (111), (100), and (110) oriented gold nanowires were prepared at $T = 0$ K and then a procedure for a wire preparation from Ref. [12] was used. Circular cross-sections with maximal radii of 0.9 and 1.2 nm were constructed. The periodic boundary conditions were applied along the axis direction. The number of atoms in MD boxes was between 566 and 1116, as shown in Table I. The temperature was controlled by rescaling particle velocities. A time step of 7.14×10^{-15} s was used. Structures were analyzed after long equilibration of $10^5 - 10^6$ time steps. Figures 1-5 show the results obtained after evolution of 10^5 time steps.

Nanowires with initial fcc(111) cross-sections are labeled as *A* and *B* in Table I. Already at low temperatures they form multiwalled structures. A nanowire *A* consists of three cylindrical walls and a thin core. The infinite nanowire *A* at 300 K has a similar structure as a finite nanowire with the same diameter simulated at this temperature and described in Ref. [10]. The same result, i.e., that only minor differences exist between finite and infinite wires, was obtained in the first principles density functional studies of monoatomic gold nanowires [15,16]. At higher temperatures ($T < 900$ K) the walls are more homogeneous than at $T = 300$ K. The structure of the nanowire *A* at $T = 800$ K is shown in Fig. 1(a). A nanowire *B* at 300 K consists of a large fcc(111) core and an outer cylindrical wall. Above 600 K this core breaks into several shells. Figure 1(b) shows that the nanowire *B* at higher temperatures consists of four cylindrical walls and a thin filled core.

Nanowires with initial fcc(110) cross-sections are labeled as *C* and *D* in Table I. The nanowire *C* consists of three shells shown in Fig. 2(a). The core of the nanowire *C* is square and empty. The multiwalled structure is less pronounced in the nanowire *D*. Figure 2(b) shows that for this nanowire the fcc structure of a core remains, although outer coaxial walls are also formed.

Simulation for initial cross-sections with the density and structure of unreconstructed Au(100) surface have shown that a strong torsion of nanowires exists. Then nanowires with the density increase in the top and bottom layers of the MD box were prepared. The density increment in these layers was taken in accordance with the properties of reconstruction on Au(100) [17,18]. Although the MD box repeats along the wire axis by the periodic boundary conditions, it was found that this density increase is sufficient to stabilize the nanowire. These nanowires with a stable untwisted cylindrical morphology are labeled as *E* and *F* in Table I. The nanowire *E* shown in Fig. 3(a) consists of three shells. The most interior of these shells is empty and square. It is interesting to point out a similarity between nanowires *C* (Fig. 2(a)) and *E* (Fig. 3(a)) at $T = 800$ K. As already explained, these nanowires evolved from different initial structures at $T = 0$ K. Figure 3(b) shows that the nanowire *F* at $T = 800$ K consists of four shells. Its core is empty, interior shells are irregular, and the walls are more disordered than in other nanowires at this temperature. The cylindrical walls in the nanowire *F* are more ordered at 900 K than at 800 K. The structure of this nanowire at 800 K was presented in Fig. 3(b) for a comparison with other nanowires.

The cylindrical shells (such as these shown in Figs. 1-3) represent radial density oscillations in nanowires. A related problem of a fluid in a finite geometry was studied within the one-dimensional lattice gas model [19]. Near the walls the layering effects were found. The inner part of the fluid behaves as a bulk if distances between the walls are large. For small

separations of the order of several interatomic distances strong density inhomogeneities appear. These density oscillations were obtained as a result of constructive and destructive interference between ordering induced by the walls. The MD boxes for nanowires consist of cylindrical gold surfaces at small radial separations which produces strong density oscillations. The layering effects are pronounced in gold, as well as in graphite and other materials for which multishelled nanostructures were observed [10]. The intershells spacings in Figs. 1-3 (and in other nanowires not shown here) are inhomogeneous and change between 0.1 and 0.2 *nm*.

All nanowires melt in the temperature interval (900 – 1100) K, i.e., well below the bulk melting temperature for this potential ($T_b \sim 1350$ K [14]). With increasing temperature highly diffusive atoms progressively appear in all cylindrical walls. Therefore, all shells melt simultaneously. The average mean-square displacements for three nanowires are presented in Fig. 4. The graphs for remaining three nanowires are similar. The displacements sharply increase at (900 – 1000) K. The diffusion coefficients have a similar temperature dependence. The liquid nanowires up to the bulk melting temperature retain a layered structure with limited interdiffusion.

Internal energy as a function of temperature for different nanowires is shown in Fig. 5. Melting is the first-order phase transition and its typical feature in three-dimensional systems is a jump in the caloric curve. In Fig. 5 the jumps in $E(T)$ are less pronounced than in Ref. [12] for the (110) oriented filled lead nanowires with radii between 1.3 and 2.5 *nm*. It is known that strict phase transitions do not exist for one-dimensional systems [20]. However, a possibility for the first-order phase transitions was studied in the one-dimensional model [21]. For this model pseudo-first-order transitions were found for the cylindrical systems with cross sections of 10 – 20 nearest neighbors units. These pseudo-transitions are indistinguishable from real ones. Simulated here multishelled gold nanowires with smaller cross sections are close to one-dimensional systems. Filled lead nanowires with larger cross sections studied in Ref. [12] are in the regime of the pseudo-first-order transitions and the jumps in $E(T)$ are apparent. Approximate finite-size scaling analysis shows that a first-order phase transition at temperature T_c in a finite system is broadened over an interval:

$$\frac{\Delta T_c}{T_c} \sim \frac{1}{N\sigma}, \quad (2)$$

where σ is the latent entropy of the bulk transition and N is the number of particles [22,23]. The latent entropy in the Eq. (2) is the ratio between a latent heat per particle and T_c , measured in units of the Boltzmann constant. The latent heat of melting for Au is 12.54 kJ/mol [24]. Equation (2) gives that the broadening of the transition for gold nanowires is $\Delta T_c/T_c \sim 10^{-3}$. Figure 5 shows that the transition is smeared over larger temperature intervals. Additional contribution to the broadening of the melting transition is given by the decrease of the latent heat with the size. The latent heat of this transition tends to disappear as the size of the system decreases. The melting of multishelled nanowires is also the structure dependent. Therefore, because of the irregularity of the shells the features of the melting transition for multishelled nanowires do not change regularly with the number of atoms.

In conclusion, a MD study of structural and melting properties for infinite gold nanowires within the framework of the embedded-atom method is presented. It was found that in all

nanowires coaxial cylindrical walls exist. The shells are the most pronounced for an initial fcc(111) orientation. The walls are the most homogeneous at (800 – 900) K. Nanowires melt around 1000 K by simultaneous melting of all shells. This study suggests the optimal temperature and the initial structure for fabrication of multishelled gold nanowires. These nanowires are important for applications in mesoscopic electronic devices. The melting of multiwalled nanowires brings an insight into a specific first-order phase transition in unusual multiwalled quasi one-dimensional structures.

ACKNOWLEDGMENTS

This work has been carried out under the CRO-MZT project 119206-“Dynamical Properties of Surfaces” and the EC Research Action COST P3-“Simulation of Physical Phenomena in Technological Applications”.

REFERENCES

- [1] U. Landman, R. N. Barnett, and W. D. Luedtke, *Z. Phys. D* **40**, 282 (1997).
- [2] H. Ohnishi, Y. Kondo, and K. Takayanagi, *Nature* **395**, 780 (1998).
- [3] A. I. Yanson, G. Rubio Bollinger, H. E. van den Brom, N. Agrait, and J. M. van Ruitenbeek, *Nature* **395**, 783 (1998).
- [4] P. Pawlow, *Z. Phys. Chem.* **65**, 545 (1909).
- [5] J. P. Borel, *Surf. Sci.* **106**, 1 (1981).
- [6] T. P. Martin, *Phys. Rep.* **273**, 201 (1996).
- [7] V. N. Bogomolov, E. V. Kolla, and Yu. A. Kumzerov, *JETP Lett.* **41**, 34 (1985).
- [8] C. Yannouleas and U. Landman, *J. Phys. Chem. B* **101**, 5780 (1997).
- [9] A. I. Yanson, I. K. Yanson, and J. M. van Ruitenbeek, *Nature* **400**, 144 (1999).
- [10] G. Bilalbegović, *Phys. Rev. B* **58**, 15412 (1998).
- [11] O. Gülseren, F. Ercolessi, and E. Tosatti, *Phys. Rev. Lett.* **80**, 3775 (1998).
- [12] O. Gülseren, F. Ercolessi, and E. Tosatti, *Phys. Rev. B* **51**, 7377 (1995).
- [13] G. M. Finbow, R. M. Lynden-Bell, and I. R. McDonald, *Mol. Phys.* **92**, 705 (1997).
- [14] F. Ercolessi, M. Parrinello, and E. Tosatti, *Philos. Mag. A* **58**, 213 (1988).
- [15] D. Sanchez-Portal, E. Artacho, J. Junquera, P. Ordejon, A. Garcia, and J. M. Soler, *Phys. Rev. Lett.* **83**, 3884 (1999).
- [16] L. De Maria and M. Springborg, preprint, cond-mat/9904181.
- [17] F. Ercolessi, E. Tosatti, and M. Parrinello, *Phys. Rev. Lett.* **57**, 719 (1986).
- [18] G. Bilalbegović and E. Tosatti, *Phys. Rev.* **48**, 11240 (1993).
- [19] P. Tarazona and L. Vicente, *Mol. Phys.* **56**, 557 (1985).
- [20] L. D. Landau and E. M. Lifshitz, *Statistical Physics*, Pergamon, Oxford (1980).
- [21] Y. Imry and D. J. Scalapino, *Phys. Rev. A* **9**, 1672 (1974).
- [22] Y. Imry, *Phys. Rev. B* **21**, 2042 (1980).
- [23] K. Binder, *Rep. Prog. Phys.* **50**, 783 (1987).
- [24] WebElements, <http://www.shef.ac.uk/~chem/webelements/>, University of Sheffield, Sheffield (1999).

TABLES

TABLE I. Geometry of investigated nanowires. The radius here is the maximal distance from the wire axis in an initial fcc structure.

Nanowire	Initial fcc cross-section	Radius (nm)	Number of atoms
<i>A</i>	(111)	0.9	588
<i>B</i>	(111)	1.2	1032
<i>C</i>	(110)	0.9	612
<i>D</i>	(110)	1.2	1116
<i>E</i>	(100)	0.9	566
<i>F</i>	(100)	1.2	952

FIGURES

FIG. 1. Structure of nanowires A (a) and B (b). The trajectory plots refer to 800 K, a time span of ~ 7 ps, and include all atoms in the slice of 4 nm along the axes of the cylindrical MD box. The geometry of all nanowires is described in the text and Table I.

FIG. 2. Structure of nanowires C (a) and D (b). The trajectory plots are prepared as in Fig. 1.

FIG. 3. Structure of nanowires E (a) and F (b). The plots are prepared as in Fig. 1.

FIG. 4. Mean-square displacements as a function of temperature for nanowires A , B , and C , after 0.714 ns of time evolution.

FIG. 5. Caloric functions, i.e., energy as a function of temperature for all nanowires. The vertical lines enclose the temperature interval (900–1100) K where nanowires melt by simultaneous melting of all shells.

This figure "Fig1.jpg" is available in "jpg" format from:

<http://arxiv.org/ps/cond-mat/0004112v1>

This figure "Fig2.jpg" is available in "jpg" format from:

<http://arxiv.org/ps/cond-mat/0004112v1>

This figure "Fig3.jpg" is available in "jpg" format from:

<http://arxiv.org/ps/cond-mat/0004112v1>

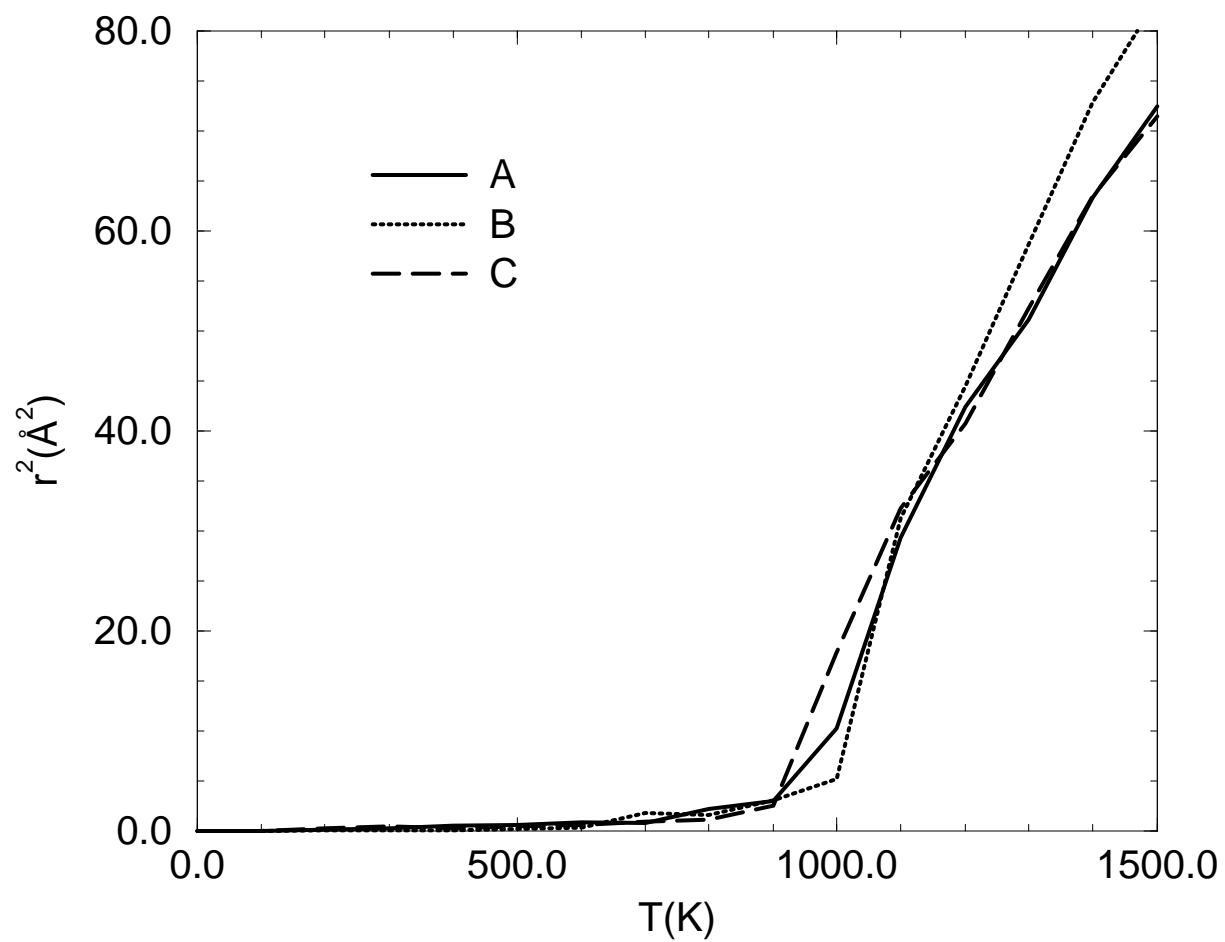


Fig. 4
G. Bilalbegovic

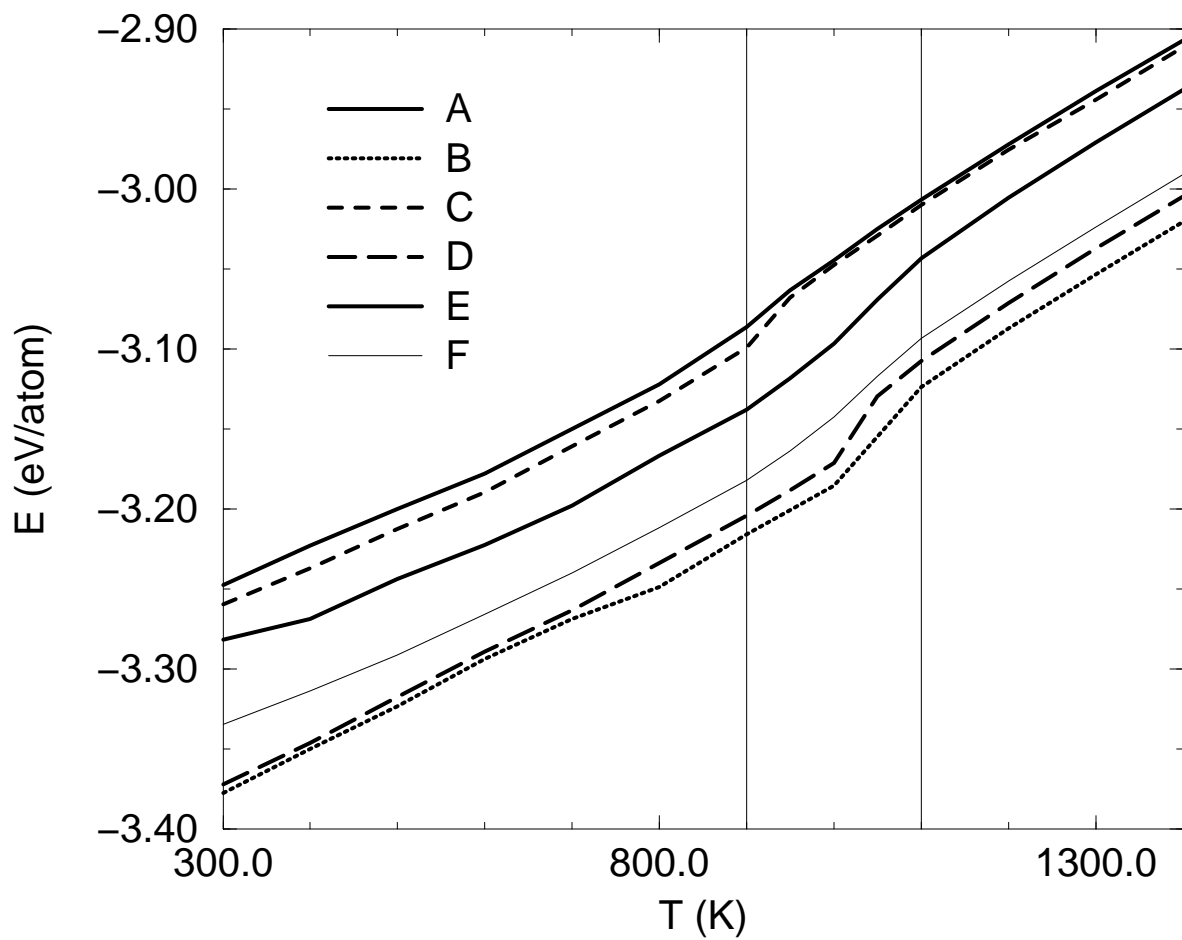


Fig. 5
G. Bilalbegovic